

Design of a TTC Antenna Using Simulation and Multiobjective Evolutionary Algorithms

Javier Moreno, Iván González, Daniel Rodríguez, University of Alcalá, Madrid, Spain

INTRODUCTION

In this paper, we present a case study about how to apply simulation–optimization, i.e., the application of simulation together with a multiobjective algorithm can help us to optimize the design parameters of an antenna with very stringent constraints. The objective is to obtain a compact dual-band helical antenna for Telemetry, Tracking, and Control (TTC) of satellites. A TTC subsystem provides the communication between a satellite and a ground station, as illustrated in Figure 1. The Telemetry system monitors the satellite retrieving its health and status of other subsystems and sending data to the station. The Tracking subsystem manages the satellite position in its orbit while the Control subsystem allows us to command the satellite, reconfiguring it if necessary. Within a TTC system, the antenna is undoubtedly the most critical part. The antenna must guarantee a proper operation within the established parameters and due to its constraints, its design can be extremely complex.

In our case study, the antenna needed to be able to operate in the S-Band at 1.81 and 2.55-GHz frequencies:

- Minimizing the cross-polarization level.
- Maximizing the gain for the Right-Hand Circular Polarization (RHCP).

In our case study, the parameters of the antenna that fulfills the radiation patterns needed for the communication are obtained using a simulation tool called MONURBS [1] together with two well-known multiobjective algorithms: Non-dominated Sorting Genetic Algorithm

Authors' current address: J. Moreno, I. González, and D. Rodríguez, Department of Computer Science, University of Alcalá, Madrid 28805, Spain, E-mail: (javier.morenom@edu.uah.es).

Manuscript received August 30, 2018, revised December 13, 2018, and ready for publication May 10, 2019.

Review handled by M. D. R-Moreno.
0885-8985/19/\$26.00 © 2019 IEEE

(NSGA-II) [2] and the Strength Pareto Evolutionary Algorithm-2 (SPEA-2) [3].

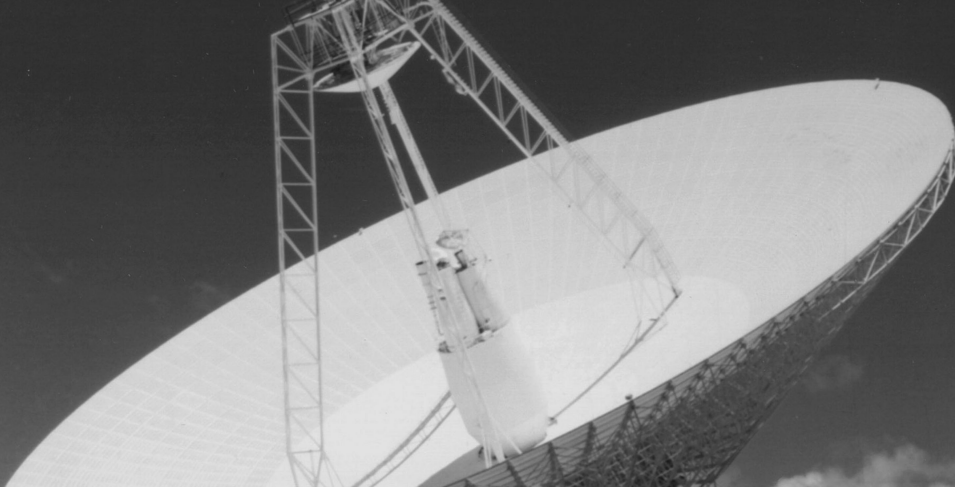
In this paper, a comparison with previous designs and the antenna prototype is presented, showing that simulation–optimization can obtain multiple valid solutions and accelerate the design process.

PREVIOUS EXPERIENCE AND MOTIVATION

In a previous work, González et al. [4] presented the design of a compact dual-band helical antenna for TTC applications in satellites. In [5], we proposed the use of NSGA-II to reduce the cost of time and optimize the design of the helical antenna. Here, we extend our proposal by applying the SPEA-2 algorithm to obtain multiple valid solutions and to expedite the process in future designs. The initial work was immersed in a ESA project 20995/NL/ST/na, "S-Band Toroidal Antenna," where the main contractor was RYMSA.¹

Although the geometric model is quite simple, it needs to be parametrized according to rigorous requirements where there are several objectives that the optimization process has to deal with. In the previous work [4], the optimization process was carried out applying the *Gradient Descent* (GD) algorithm with a simulation tool called MONURBS to analyze and obtain the radiation pattern of the antenna. This GD method was used with a cost function that depended on the antenna requirements. However, it resulted in a very complex problem with a large number of maximums and minimums where the application of the GD method was difficult and not appropriate (it was more like a random sampler in the search space). A huge number of simulations were needed to obtain a valid solution that satisfied all the requirements simultaneously. It was, therefore, an extremely CPU intensive task that needed a very large time span (several months). As a consequence, we started tackling this problem as a case study applying multiobjective optimization techniques.

¹ <http://www.tryo.es/>



Although there are a large number of multiobjective algorithms, we selected the two most popular and well-known ones, NSGA-II and SPEA-2, for our case study. Both algorithms are by far the most popular and referenced in the multiobjective literature.

PROBLEM DEFINITION

For the purpose of optimization, we can divide the problem into two parts:

- (1) The problem parameters, which define the antenna geometry.
- (2) The problem objectives, which define how good is the antenna according to the specified requirements.

A helix antenna is formed by one or more strips wrapped helically. The geometrical model of a helix antenna is defined by a truncated cone. The antenna has four rolled strip in the form of a helix from the bottom circle to the topside circle. The strips are short-circuited in the top of the antenna. Finally, a post is set internally to the four strips to be mechanically strong enough. Therefore, the antenna geometry can be defined by four parameters (see Figure 2):

- Bottom radius (r).
- Top radius (R).
- Height (h).
- Number of turns of the helix (t).

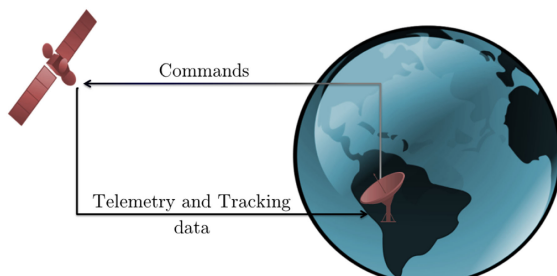


Figure 1.
TTC communication system.

The most important electromagnetic requirements were stated as follows:

- Dual Band operation at 1.81 and 2.55 GHz in the S Band (two frequencies).
- RHCP, the main electrical field that radiates the antenna.
- Peak maximum gain greater than 2 dBi for the RHCP polarization.
- Minimum gain of 0 dBi in the range coverage for the RHCP polarization.
- Cross-polarization level had to be smaller than -12 dB (difference between LHCP—Left Hand Circular Polarization—and RHCP), this is difficult to obtain.
- The above specifications in an equatorial radiation pattern had to be satisfied in the elevation angle with a range between 70° and 110° .

Figures 3 and 4 show these requirements graphically. The mask has to be satisfied for radiation pattern in the desired

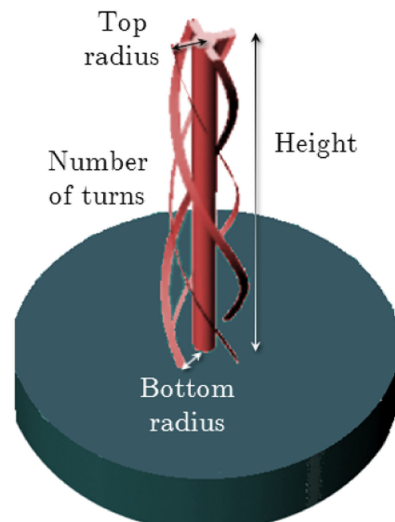


Figure 2.
Geometrical parameters of a helical antenna.

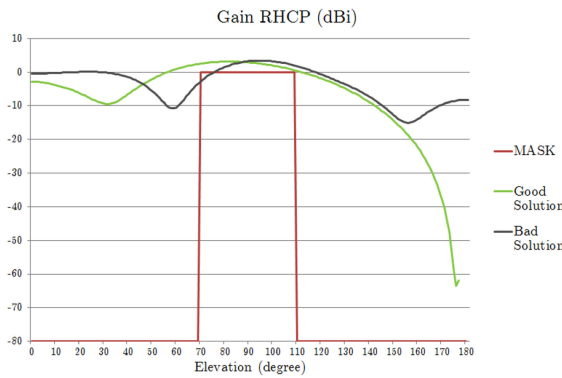


Figure 3.
Gain objective.

directions for the main (RHCP) as well as for the cross-polar components (difference between LHCP-RHCP).

Additionally, the weight of the prototype had to be as small as possible, therefore it was important to reduce the volume of the antenna. The volume of the antenna can be calculated using the truncated cone volume formula:

$$v = \frac{1}{3} \cdot \pi \cdot h \cdot (R^2 + r^2 + R \cdot r). \quad (1)$$

Due to the difficulty of the problem, we decided to take out the volume requirement of the optimization process. The problem objectives will be:

- Maximize the RHCP gain for 1.81-GHz frequency.
- Minimize the cross-polar polarization level for 1.81-GHz frequency in the range between 70° and 110°. In this range, gain must be above 0 dBi.
- Maximize the RHCP gain for 2.55-GHz frequency.
- Minimize the cross-polar polarization level for 2.55-GHz frequency in the range between 70° and 110°. In this range, gain must be above 0 dBi.

Once the optimization process ends, solutions that meet all requirements are filtered and the volume of each solution is computed.

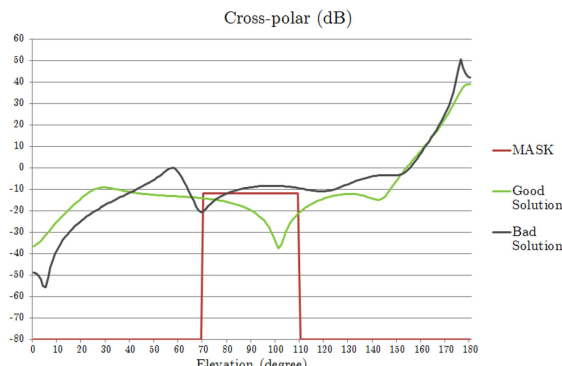


Figure 4.
Cross-polar objective.

Finally, joining problem parameters and problem objectives, we define a *problem solution* or simply a *solution* s , as a tuple of two vectors, $s = (s_p, s_o)$, where:

- s_p defines the four geometric parameters, i.e.: $s_p = (s_{p1}, \dots, s_{pn}) : m = 4$.
- s_o defines the four radiation objectives, i.e.: $s_o = (s_{o1}, \dots, s_{on}) : n = 4$.

THEORETICAL BACKGROUND

ANALYSIS OF ANTENNAS: NUMERICAL METHODS

Before manufacturing, the antenna must be designed and optimized to satisfy the requirements that have been imposed in Section "PROBLEM DEFINITION." This is not an easy task, because the antenna is not a canonical object and there is not a simple formula that can be used to obtain the radiation parameters. Then, it is necessary to apply advanced numerical methods in computers to obtain the behavior of the antenna under test. These numerical methods are known as computational electromagnetics methods (CEM) [6] and they are applied to a variety of complex problems: antennas, radar cross section (RCS), propagation, radomes, electromagnetic compatibility, communications, etc.

When an electromagnetic signal impinges with an object or is used to feed a structure like an antenna, then a current is induced on it generating an electromagnetic field that is radiated in all the space. This is known as the scattering phenomena. This phenomena follows the Maxwell Equations [7] that relate the time domain and spatial variation of the electric and magnetic field generated by the currents. To solve these equations, several advanced numerical techniques were developed as can be seen in Figure 5.

Every technique has its own advantages and disadvantages, but the question is which method is used to solve this problem? Mainly, this depends on the size of the object compared with the frequency of operation. According to the main classification of Figure 5, there are basically two:

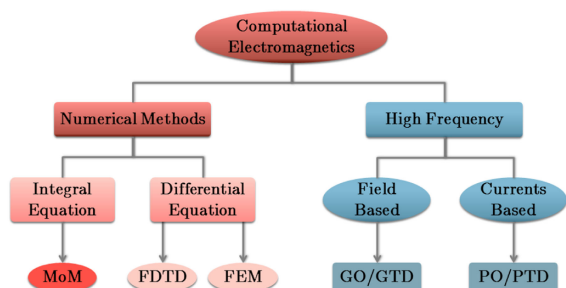
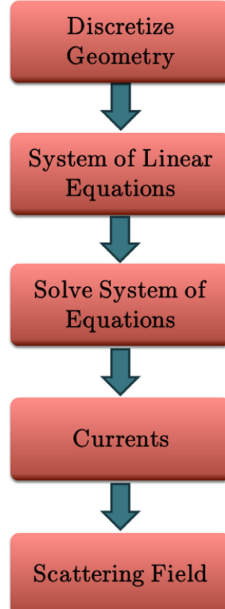
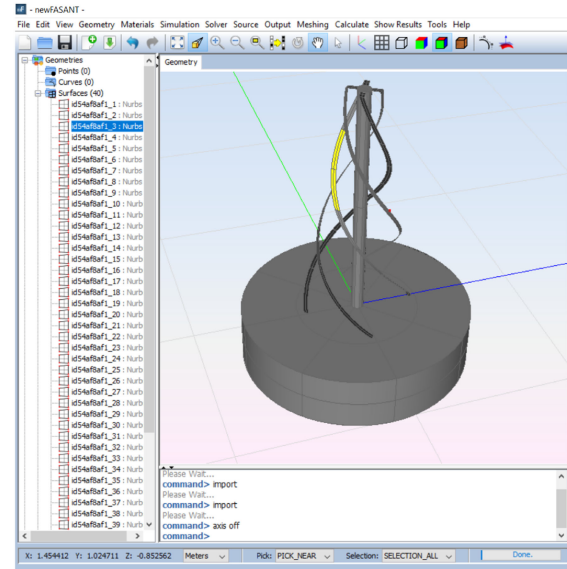


Figure 5.
Classification of numerical techniques.

**Figure 6.**

Analysis of the antenna using the MoM technique.

- High Frequency methods (Asymptotic Methods), where it is necessary that the object must be electrically large compared with the frequency (about several wavelengths). This is an approximation of the Maxwell equations, and in this case the current is assumed to be local character, that is, the current in one part of the structure is independent of other part, there is not coupling between structure parts. This is not the case, because at 2 GHz the wavelength is 0.15 m and the antenna size is close to this value. The techniques than can be used in this classification are Geometrical Optic (GO) [8] combined with the Geometrical Theory of Diffraction (GTD) [9] that are based on obtaining the Electrical Field of every ray that impinges the structure; and the Physical Optic (PO) [10]/Physical Theory of Diffraction (PTD) [11] that are based on calculating the currents on the object to obtain after the scattering field.
- Numerical Methods (Rigorous Methods), which does not matter the size of the object compared with the frequency, but they have the problem that when the frequency increases, more computation resources (memory and CPU) are needed. The main characteristic of the currents of the object is they are strongly coupled with other parts of the object. Mainly there are three techniques depending on the kind of Maxwell Equations they are using: Moment of Methods (MoM) [12] that solves the integral Maxwell Equations, and Finite Elements (FEM) [13], and Finite Difference Time Domain (FDTD)

**Figure 7.**

Example of geometrical model of the antenna and a NURBS selected.

[14] that solves the differential partial Maxwell equations. These techniques can be applied to this case without any problem, and we have chosen MoM because this is the technique that the Electromagnetic Computing Group (GEC) [15] has been working to solve electromagnetic problems for more than 20 years.

When the object has arbitrary shape, there is not analytic solution as has been mentioned before. Then, a numerical technique must be applied to solve the problem. The MoM technique has to be selected and it is going to be applied to the analysis of the antenna. The process that is going to be applied to the analysis of the antenna is shown in Figure 6.

The geometrical model of the antenna is represented using Non-Uniform Rational B-Splines [16] (see Figure 7), a kind of parametric surfaces that are very common to model complex objects with a little information that are able to represent very accurately the real shape of the object, avoiding the use of planar facets models that are not so good when curved surfaces are presented. In this example of antenna, with only 40 NURBS surface is enough to represent the geometry.

The Maxwell equation cannot be applied directly to the geometrical model of the antenna, so a first step of discretization of the geometry must be done. This is done using a mesher [17], a code that preprocess and discretize the geometry obtaining small pieces of the surfaces named elements. The elements shall have a size lower than the wavelength, typically an edge size between wavelength/8 or wavelength/10 to obtain an accurate representation of the current. Thus, it can be seen that when the object of

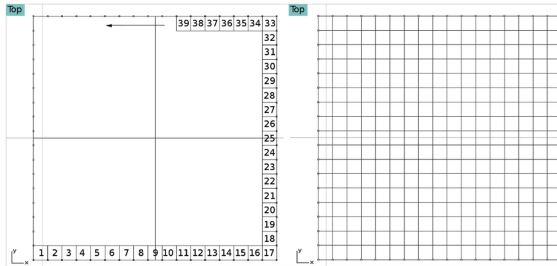


Figure 8.
Example of discretization procedure.

the size is bigger or the frequency is increased, more elements are needed and then more computational resources would be necessary. The discretization process is done according to the Paving Technique [17] that is based on dividing the edges of the surfaces according to the previous size and then fill the original surface with quadrangular elements from the edges to the inner part of the surface. Figure 8 shows an example of the Paving algorithm apply to a plane surface where 289 elements have been obtained.

The right image of Figure 8 is the mesh of the surface and it is very important that the mesh is continuous and the elements have more or less the same size and not be an irregular mesh. It is so important to have a good mesh as to apply an accurate numerical technique to obtain good results. Figure 9 shows the continuous mesh obtained with the mesher when it has been applied to the helix antenna.

When the elements have been obtained, it is necessary to define the basis functions that will model the current on the element, the amplitude of these basis functions will be the unknown current that will be necessary to calculate. The unknowns or subdomains will be defined by two elements that share a common edge. This common edge

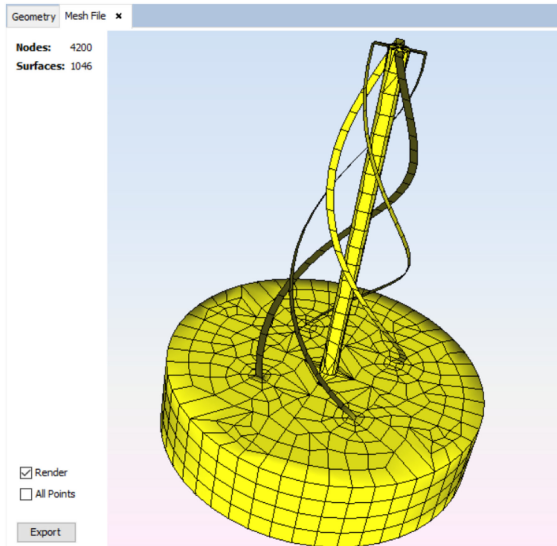


Figure 9.
Mesh of the helix antenna.

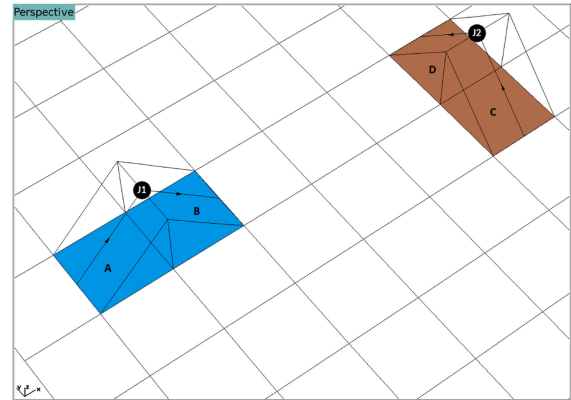


Figure 10.
Definition of the subdomains or current elements.

will have the maximum of the amplitude current and will be the part of the geometry where the Maxwell equation will be applied to build the System of Linear Equations. Thus, a basis function will be defined as a conformed rooftop that models the current that flows on the subdomain. The current starts from one edge of the first element, reach the maximum on the common edges of both elements and ends in the edge of the second element. Figure 10 shows the definition of the basis function between two elements that share a common edge. Elements A and B define a current element where the J1 amplitude of the current is unknown and the elements C and D define another current element where the amplitude J2 is unknown. The J1 is a current element according to X direction and J2 according Y. In both elements, it can be seen that the current is born in patch A or C and the current dies in element B or C depending on the subdomain considered.

Figure 11 shows all subdomains obtaining from the mesh of the helix antenna. In this example, there are 1929 subdomains or current elements where the Maxwell equation will be applied and a linear system of 1929 equations with 1929 unknowns must be solved to know the amplitude of the currents and then to be able to calculate the scattering field to obtain the radiation patterns.

The equation that must satisfy every subdomain of the antenna must be the Electric Field Integral Equation (EFIE) [7], [12] that has the following expression when the surfaces of the geometry are Perfect Electrical Conductors (PEC):

$$\hat{n} \times \vec{E}^{\text{imp}} = \left[\hat{n} \times \frac{j\omega\mu}{4\pi} \iint_S \vec{J}_S(\vec{r}') G(\vec{r}, \vec{r}') dS' \right. \\ \left. + \frac{j}{4\pi\omega\epsilon} \nabla \iint_S \nabla' \cdot \iint_S \vec{J}_S(\vec{r}') G(\vec{r}, \vec{r}') dS' \right] \quad (2)$$

where \vec{E}^{imp} is the impressed electrical field (electrical field that feed the antenna), \hat{n} is the normal vector on every surface point, $\vec{J}_S(\vec{r}')$ is the current density defined in every

Perspective

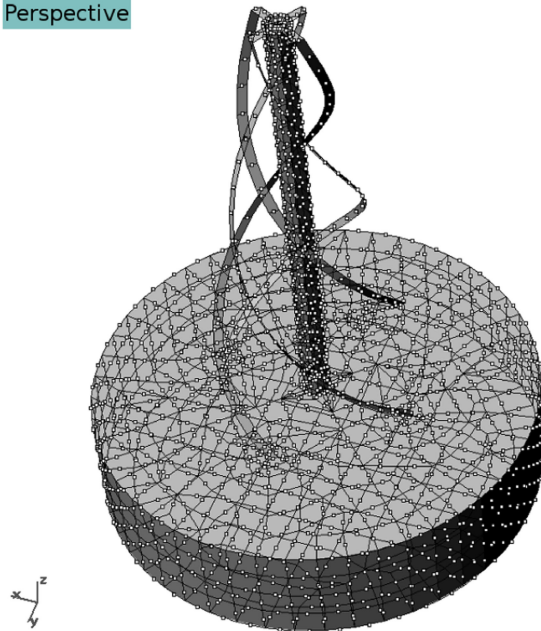


Figure 11.
Subdomains obtained from the mesh for the helix antenna.

subdomain, and $G(\vec{r}, \vec{r}')$ is the green function that gives an idea that how a subdomain (\vec{r}') couples with other subdomain (\vec{r}). Each subdomain couples with the other subdomains and this defines a system of equations of this way

$$[Z][I] = [V] \quad (3)$$

where $[Z]$ is the coupling matrix of $N \times N$ elements, where every element is known, $[I]$ the unknown amplitudes of the currents, vector of N elements, and $[V]$ is the independent term, a vector of N elements that it is known and depends on the impressed electrical field. Then, the amplitude of the currents can be obtained solving the system with direct methods, for instance, inverting the matrix $[Z]$ or with iterative methods like Biconjugate Gradient Stabilized Method (BICGSTAB) [18] or Generalized Minimal Residual Method (GMRES) [19].

To feed the helix antenna, it is necessary to fix an impressed voltage in every helix with a difference of phase of 90° . Thus, in this way, the RHCP or LHCP can be obtained. Figure 12 shows the location of the impressed voltage between the bottom end of every helix and the top lid of the cylinder. In the right of the figure, the voltage values are assigned in this way.

When the system of equations has been solved, the currents can be visualized as in Figure 13. Red color shows where the amplitude is maximum. These currents will scatter the electrical and magnetical field of the antenna.

When the amplitudes of the currents are known, then all the scattering fields of the antenna can be obtaining in every part of the space, according to the following

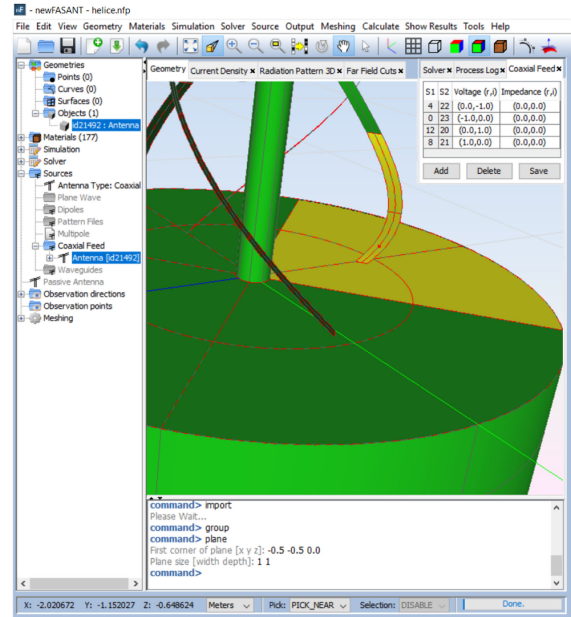


Figure 12.
Assign of the impressed voltage to every helix.

expression in far field region [7]:

$$\vec{E}^{\text{scatt}}(\vec{r}) = -\frac{j\omega\mu}{4\pi} \frac{e^{-jkr}}{r} \iint_S \vec{J}_S(\vec{r}') e^{-jk\hat{r}\cdot\vec{r}'} dS'. \quad (4)$$

Figure 14 shows the 3-D radiation pattern when the equatorial radiation pattern can be noticed.

MULTIOBJECTIVE OPTIMIZATION PROBLEMS

Multiobjective Optimization Problems (MOOP) are those that involve multiple and conflicting objective functions.

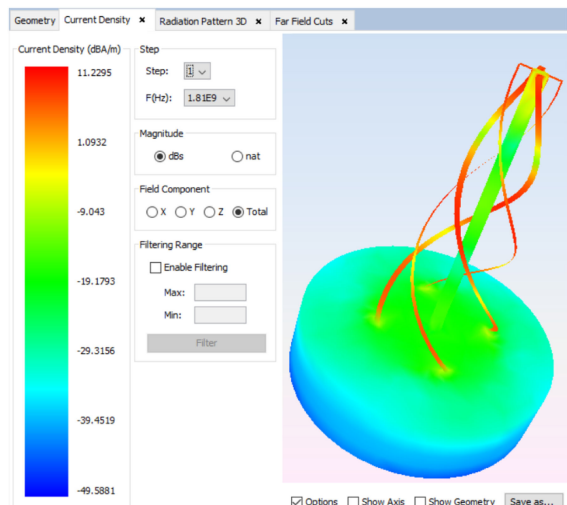
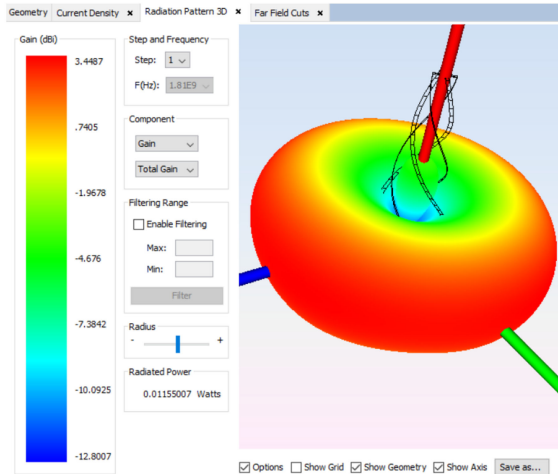


Figure 13.
Current distribution of the antenna.


Figure 14.

3-D radiation pattern of the antenna.

In general, there are multiple valid solutions that are defined using the concept of *Pareto-optimal Front*. The Pareto-optimal Front is the set of the best possible solutions for the problem. In Section “PROBLEM DEFINITION,” we defined the solution objectives s_o as a vector of n objective values, i.e., $s_o = (s_{o_1}, \dots, s_{o_n})$. To obtain the Pareto-optimal Front of a problem, it is necessary to sort all solutions according to their relationship of dominance. We say that a solution s dominates a solution v , denoted as $s \preceq v$ if the objective values of s are partially less (at least one less and equal the rest) than the objectives values of v , i.e., $\forall i \in (1, \dots, n), s_{o_i} \leq v_{o_i} \wedge \exists i \in (1, \dots, n) : s_{o_i} < v_{o_i}$. This definition considers that we are minimizing all objective values. To maximize, just change the less than operator by greater than operator. Note that the relationship of order \preceq is partial and therefore there may be solutions that do not dominate each other. A set of solutions that do not dominate each other is said to belong to the same front. Those solutions that are not dominated by any other, belong to the first front, called

Pareto-optimal Front. The solutions dominated by those belonging to the first front, but which do not dominate each other, form the second front. And so, successively, all the solutions are grouped in different fronts. To illustrate the previous concepts, let us provide an example with the problem that concerns us. In our case, we have four objectives to optimize, i.e., cross-polar polarization level (dB) and gain RHCP (dBi) for 1.81 and 2.55-GHz frequencies. Table 1 shows the objective values of six solutions obtained from the experimentation. Solutions 1 and 2 correspond to solutions SPEA-2 5 and SPEA-2 6 shown in Table 2. Last column of the table shows the front to which each solution belongs. All solutions in the first front belong to the Pareto-optimal Front.

Note that solutions in the same front do not dominate each other, but they do dominate solutions in lower fronts. Solution 1, for example, dominates solution 2 for the 1.81-GHz values, but is dominated for the 2.55-GHz values by solution 2. Figure 15 shows a 4-D chart (the fourth axis is the color range) with values obtained from the experimentation (some of them are shown in Table 1). Solutions in the Pareto-optimal Front (front 1) correspond to the most top-left plane.

METAHEURISTICS AND EVOLUTIONARY ALGORITHMS

Metaheuristics are a family of approximate optimization techniques for solving the computational problem. There are multiple metaheuristic techniques available for solving MOOPs.

Evolutionary algorithms (EAs) are a set of algorithms inspired in the biologic evolution. Algorithm 1 shows the pseudocode of a standard EA. At each generation (loop iteration), an auxiliary population (with the same size as the original one) is generated by iteratively applying the genetic operators (crossover and mutation), then, both the current and the auxiliary populations are merged into one single new population. Worst individuals of the new

Table 1.

Objective Values of Six Solutions					
Solution	Cross Polar Level (dB)		Gain RHCP (dBi)		Front
	1.81 GHz	2.55 GHz	1.81 GHz	2.55 GHz	
1	-19.13	-13.82	5.81	3.82	1
2	-12.87	-19.2	3.33	4.02	1
3	-9.2	-8.83	-1.7	-3.1	2
4	-5.9	-9.01	-5.2	-5.0	2
5	-1.3	-5.2	-8.2	-5.1	3
6	-3.9	-0.4	-5.3	-9.75	3

Table 2.**Parameters of Best Solutions Found by Using jMetal and MONURBS**

Algorithm	Turns	Bottom radius (cm)	Top radius (cm)	Height (cm)	Volume (cm ³)
Gradient Descent	0.831	1.945	1.022	13.8	98.49
NSGA-II 1	0.787	2.458	1.001	13.732	136.672
NSGA-II 2	0.787	2.339	1.02	13.732	127.915
NSGA-II 3	0.787	2.458	1.001	13.732	136.672
NSGA-II 4	0.791	2.458	1.001	14.505	144.346
NSGA-II 5	0.777	1.929	1.145	14.072	106.676
NSGA-II 6	0.787	2.339	1.02	13.732	127.915
NSGA-II 7	0.777	1.929	1.145	14.072	106.676
SPEA-2 1	0.859	2.409	0.701	14.433	120.677
SPEA-2 2	1.119	2.168	0.734	16.898	120.837
SPEA-2 3	0.782	2.385	0.709	14.859	122.676
SPEA-2 4	0.801	2.494	0.748	14.697	133.022
SPEA-2 5	0.84	1.032	0.753	13.593	34.281
SPEA-2 6	0.637	1.092	0.72	13.275	34.701
SPEA-2 7	0.637	1.344	0.704	13.145	44.739

population are removed (i.e., the best solutions are selected), until the size of the new population is reduced by half. For us, each individual is a problem solution, so individual and solution are equivalent concepts.

EAs are particularly desirable to solve MOOPs, primarily because of their population-based nature. This enables them to capture the dominance relations in the

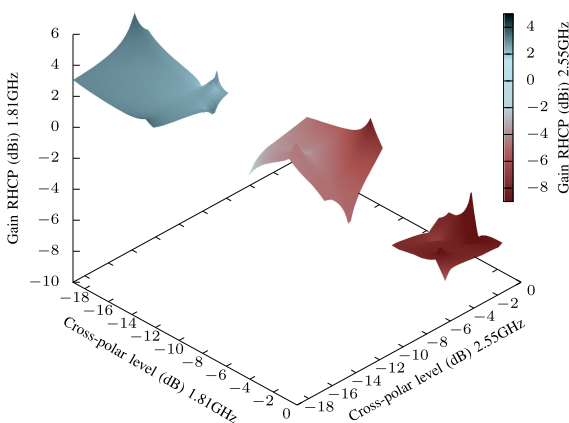
population as a way to guide the search toward the Pareto-optimal Front.

EAs usually contain several parameters that need to be tuned for each particular application at the same time considering:

- (1) Nonconflicting objectives, i.e., achieve a single optimal solution satisfies all objectives simultaneously.
- (2) Competing objectives, i.e., cannot be optimized simultaneously.

In addition, since the EAs are stochastic optimization techniques, different runs tend to produce different results. Therefore, multiple runs of the same algorithm on a given problem are needed to statistically describe their performance on that problem. For a more detailed discussion of the application of EAs in multiobjective optimization, the reader is referred to Coello et al. [20] and Deb et al. [2]. Multiobjective EAs need to fulfill two primary roles:

- (1) Guiding the search toward the Pareto-optimal Front set to accomplish optimal or near-optimized solutions.
- (2) Maintaining a diverse population to achieve a well-distributed nondominated front, thereby fully exploring the solution space.

**Figure 15.**

Four-dimensional representation of solutions obtained in the experimentation.

Algorithm 1: Evolutionary Algorithm

```

1: Create random initial population  $P$ 
2: Evaluate population  $P$ 
3: while Stopping criteria not reached do
4:   Select population  $P$ 
5:   Create empty population  $Q$ 
6:   for Population size/2 times do
7:     Select two parents from  $P$ 
8:     Perform crossover & Mutation
9:     Insert children into  $Q$ 
10:  end for
11:  Evaluate population  $Q$ 
12:   $P \leftarrow Q$ 
13: end while
14: return  $P$ 

```

**THE NONDOMINATED SORTING GENETIC ALGORITHM-II
(NSGA-II)**

This algorithm was developed by Deb et al. [2] as an extension of an earlier proposal by Srinivas and Deb [21].

The population individuals (solutions) are evaluated (i.e., they are assigned fitness values) in relation to how close they are to the *Pareto-optimal Front* and a *crowding measure*.

The NSGA-II algorithm also considers the sparsity (density) of the individuals belonging to the same rank using a crowding measure (the Manhattan distance among individuals), with the idea of promoting diversity within the fronts (the larger the sparsity, the better). In addition, the NSGA-II includes elitism in order to maintain the best solutions from the *Pareto-optimal Front* found. The rank of each individual is based on the level of nondomination. Therefore, each solution has two attributes: i) nondomination rank (front to which the solution belongs) and ii) crowding distance. In other words, between two solutions with differing nondomination ranks, the solution with the lower rank is preferred. Otherwise, if both solutions belong to the same front, then the solution that is located in a less crowded region is preferred. The pseudocode of NSGA-II is shown in Algorithm 2. Note that lines 2 and 6 are calls to the simulator to evaluate the solution parameters. NSGA-II sends the parameters of the solution to the simulator and the simulator returns the objective values for that solution.

STRENGTH PARETO EVOLUTIONARY ALGORITHM-2 (SPEA-2)

This algorithm was proposed by Zitzler et al. [3]. In this algorithm, the strength of an individual is defined in terms of the number of solutions it dominates in the population. A fitness value is assigned to every individual, and it is defined as the sum of its strength raw fitness and a density estimation. The algorithm evolves the population through the iterative application of the variation operators on the solutions. All generated nondominated solutions are stored in an external archive. After every iteration, all nondominated

solutions (from both the population and the archive) are copied into a new generation population. If its size is larger than the population size, the algorithm applies a truncation operator to discard solutions. It is based on the distances to the k^{th} nearest neighbors (a crowding measure), so that those solutions having the largest distances to the other solutions (i.e., the most isolated ones) are selected. Algorithm 3 presents a pseudocode of SPEA-2. Note that lines 4 and 5 are calls to the simulator to evaluate each solution parameters. SPEA-2 sends the parameters of the solution to the simulator and the simulator returns the objective values for that solution.

DESIGNING THE ANTENNA

In order to obtain the radiation patterns of the antenna shown in Figure 2, it is necessary to use a simulation computer program with the input of the four parameters of the antenna, then does:

- (1) builds the geometrical model of the antenna;
- (2) discretize the model according the wavelength;
- (3) simulates the antenna to obtain the radiation patterns for both frequencies in order to be processed by the multiobjective algorithms.

Figure 16 shows the block diagram of the electromagnetic simulation stage.

The geometrical model is built using a software by which the previously stated parameters can create a geometrical file in AutoCAD DXF (Drawing Interchange Format) [22] with the surfaces that define the antenna. This file must be previously processed to be simulated with a mesher that discretize the antenna parameters as input to the simulator that calculates the radiation pattern using a simulation software called MONURBS [1].

This simulation software is being developed by the Electromagnetic Computing Group, University of Alcalá, and it is included in as part of an electromagnetic suite, newFASANT [23]. This suite can be used in many applications like electromagnetic field analysis of any complex 3-D structures such as reflectors, horns, microstrip passive devices, periodical structures, antenna on board, etc. Also, the RCS of complex platforms with arbitrary materials and the compatibility between different devices mounted on the same platform. Figure 17 shows the User Interface of the code with all the modules that can be used for several electromagnetic applications.

From this suite, the MONURBS and mesher code have been extracted and used as a black box to implement the procedure of Figure 16. The MONURBS code is based on the Moment Method Technique (MoM) that is a full-wave solution. When the object to be analyzed is large, this technique is both CPU and memory consuming and cannot

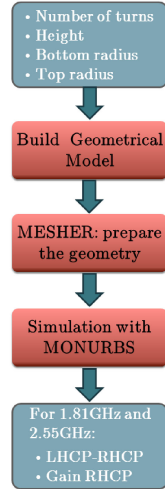


Figure 16.
Electromagnetic simulation stage block diagram.

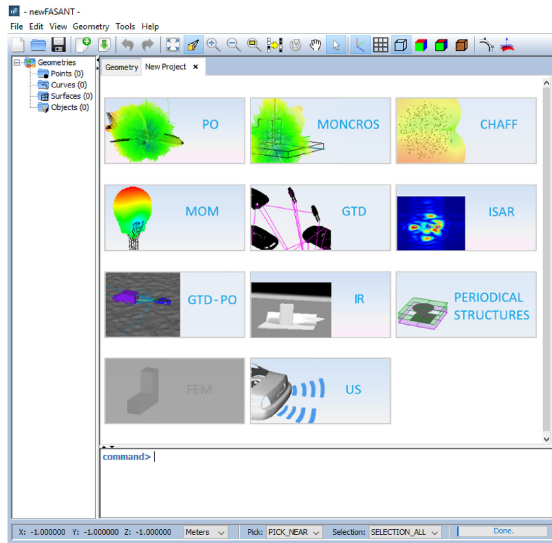


Figure 17.
Electromagnetic suite newFASANT.

be applied if the resources of the machine are not high. To overcome this, several techniques have been implemented to speed up the simulation while using less memory: (i) Fast Multipole Multilevel Method [12], [24] and (ii) the Characteristics Basis Function Method [25], [26]. Also, the Message Passing Interface (MPI) and OpenMP paradigms have also been implemented to solve the problem using less CPU time with multiprocessor machines [27].

LOOKING FOR THE OPTIMAL PARAMETERS

In this paper, we used the implementation of NSGA-II and SPEA-2 provided in the jMetal² framework [28] for

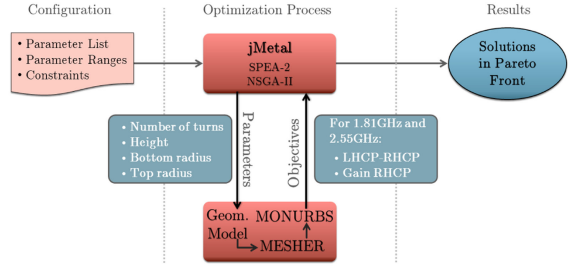


Figure 18.
Antenna parameters optimization.

multiobjective optimization together with a simulation software of antenna radiation, MONURBS, as previously described.

Algorithm 2: NSGA-II Algorithm [2]

```

1:  $P \leftarrow \text{makeInitialRandomPopulation}()$ 
2:  $P \leftarrow \text{antennaSimulator}(P)$   $\triangleright$  Call to evaluate  $P$ 
3:  $t \leftarrow 0$ 
4: while  $t \leq \text{max\_generations}$  do
5:    $Q \leftarrow \text{makeNewPopulation}(P)$ 
6:    $Q \leftarrow \text{antennaSimulator}(Q)$   $\triangleright$  Call to evaluate  $Q$ 
7:    $R \leftarrow P \cup Q$   $\triangleright$  Combine parents and offsprings
8:    $\mathcal{F} \leftarrow \text{fastNonDominatedSort}(R)$   $\triangleright$  Calculate Fronts
9:    $P \leftarrow \emptyset \wedge i \leftarrow 1$ 
10:  while  $|P| + |\mathcal{F}_i| \leq N$  do
11:     $P \leftarrow P \cup F_i$   $\triangleright$  Add  $i^{th}$  rank to population
12:     $i \leftarrow i + 1$ 
13:  end while
14:  if  $|P| \neq N$  then
15:     $\text{crowdingDistance}(\mathcal{F}_i)$   $\triangleright$  Calc. crowding measure in  $\mathcal{F}_i$ 
16:     $P \leftarrow P \cup \text{bestCrowdingSolutions}(\mathcal{F}_i, |P| - N)$ 
17:  end if
18:   $t \leftarrow t + 1$ 
19: end while
20:  $\mathcal{F} \leftarrow \text{fastNonDominatedSort}(R)$ 
21: return  $\mathcal{F}_1$   $\triangleright$  Return first front; i.e., Pareto-optimal Front

```

As jMetal is being developed in Java, the communication is also handled using the Java runtime API to simulate the antenna radiation using the antenna parameters generated by the multiobjective algorithms. Therefore, to perform the data exchange between jMetal and MONURBS, it was necessary to implement a specific method, called *AntennaSimulation(P)* (Algorithm 4) to perform the population evaluation. The calls are carried out in lines 2 and 6 in the NSGA-II (Algorithm 2), and lines 4 and 5 in the SPEA-2 (Algorithm 3). Figure 18 illustrates the communication between jMetal and MONURBS implemented in Algorithm 4.

² <https://github.com/jMetal/>

Algorithm 3: SPEA-2 Algorithm [3]

```

1:  $P_0 \leftarrow \text{makeInitialRandomPopulation}()$ 
2:  $Q_0 \leftarrow \emptyset$                                  $\triangleright$  Initial empty archive of size  $M$ 
3: while  $t \leq \text{max\_generations}$  do
4:    $P_t \leftarrow \text{antennaSimulator}(P_t)$   $\triangleright$  Call to evaluate  $P_t$ 
5:    $Q_t \leftarrow \text{antennaSimulator}(Q_t)$   $\triangleright$  Call to evaluate  $Q_t$ 
6:    $Q_{t+1} \leftarrow \text{copyNonDominatedSolutions}(P_t, Q_t)$ 
7:   if  $|Q_{t+1}| > M$  then  $\triangleright$   $Q_{t+1}$  exceeds archive size
8:      $Q_{t+1} \leftarrow \text{truncate}(Q_{t+1})$ 
9:   else if  $|Q_{t+1}| < M$  then  $\triangleright$  Fills with dominated
    solutions
10:     $Q_{t+1} \leftarrow \text{copyDominatedSolutions}$ 
         $(P_t, Q_t, M - |Q_{t+1}|)$ 
11:   end if
12:    $P_{t+1} \leftarrow \text{selectPopulation}(Q_{t+1})$   $\triangleright$  Mating selection
13:    $P_{t+1} \leftarrow \text{variationOperators}(P_{t+1})$        $\triangleright$  Apply
        recombination and mutation
14:    $t \leftarrow t + 1$ 
15: end while
16:  $\mathcal{F} \leftarrow \text{copyNonDominatedSolutions}(Q)$ 
17: return  $\mathcal{F}$                                  $\triangleright$  Return the Pareto-optimal Front

```

Algorithm 4: antennaSimulator(P)

```

1: for each solution  $s$  in population  $P$  do
2:   if  $s$  does not violates problem constraints then
3:     Invoke MONURBS process with  $s$  parameters ( $s_p$ 
   vector)
4:     Wait until MONURBS process finalizes
5:     Parse MONURBS return
6:     Update  $s$  evaluation values ( $s_o$  vector)
7:   end if
8: end for
9: return  $P$ 

```

RESULTS

In this section, we show solutions found by both i) using MONURBS (as standalone tool using its built-in *GD* optimizer) and ii) combining MONURBS and jMetal. The computer and software used to carry out the experimentation were:

- Windows Server 2016 Standard, 64 bits.
- Java version: 1.8.0-121, 64 bits.
- 8 Quad-Core AMD Opteron Processor 8356 2.29 GHz.
- 256 GB of RAM memory.

The configuration of the problem ranges, i.e., the antenna parameters was

- Number of turns: [0.2, 3].
- Bottom radius: [0.1 cm, 50 cm].

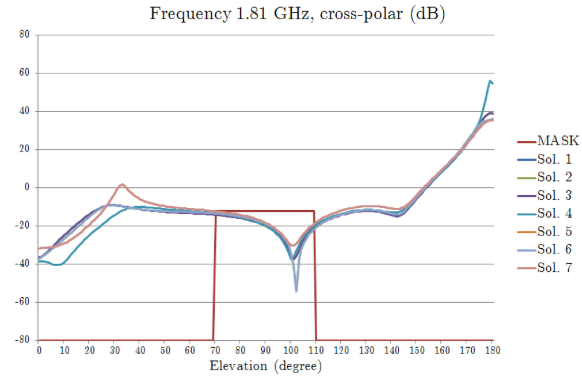


Figure 19.

1.81-GHz cross-polar objective results using NSGA-II.

- Top radius: [0.1 cm, 50 cm].
- Height: [0.1 cm, 50 cm].

Also, the configuration of NSGA-II and SPEA-2 was as follows:

- Population size: 50.
- Maximum number of algorithm iterations: 5000
- Crossover operator: Simulated binary crossover
 - Crossover probability: 90%
 - Crossover distribution index: 20.
- Mutation operator: Polynomial mutation
 - Mutation distribution index: 20
 - Mutation probability: 25%.

The results are shown in Table 2. The first column shows the solutions found by each algorithm. Four next columns show the parameters defined by each solution and the last column shows the volume of the antenna. All results were rounded to three decimals. As it can be observed, all solutions found are very close to each other, especially those obtained by NSGA-II where some of them are practically equivalent. The first row shows the result obtained with the MONURBS *GD* in order to compare such results with the ones obtained by the NSGA-II and SPEA-2 algorithms in the next rows. Figures 19 to 26 show the objective values graphically. It can be observed that all solutions met the constraints defined for this problem. The results obtained by SPEA-2 are better dispersed than those obtained by NSGA-II. Please note that the best solution obtained by SPEA-2 reduces the volume of the solution obtained using *GD* by 35%. Figure 27 shows the geometrical model of this solution. With this new approach, the CPU time to obtain a suitable solution has been reduced considerably. The solution obtained with *GD* took several months, while using NSGA-II or SPEA-2 have taken three weeks. In a future work, we will need to apply other multiobjective algorithms and techniques to explore if there are other parameters that are significantly different.

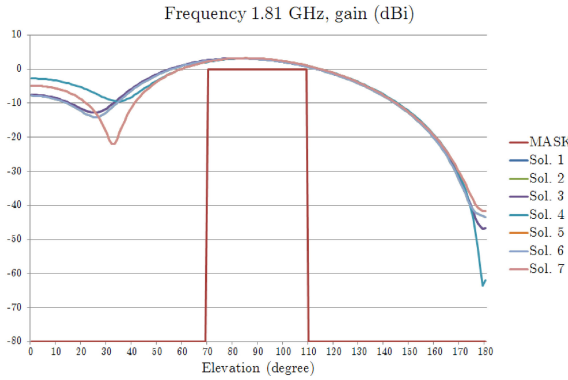


Figure 20.
1.81-GHz gain objective results using NSGA-II.

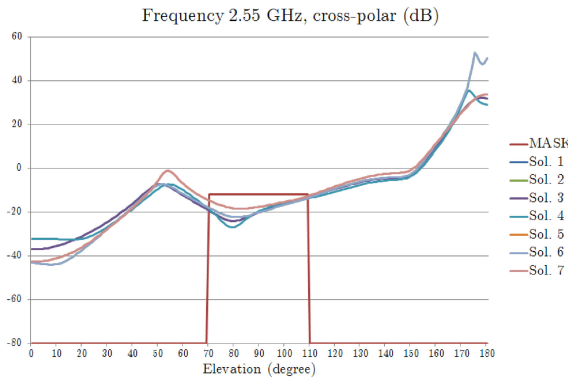


Figure 21.
2.55-GHz cross-polar objective results using NSGA-II.

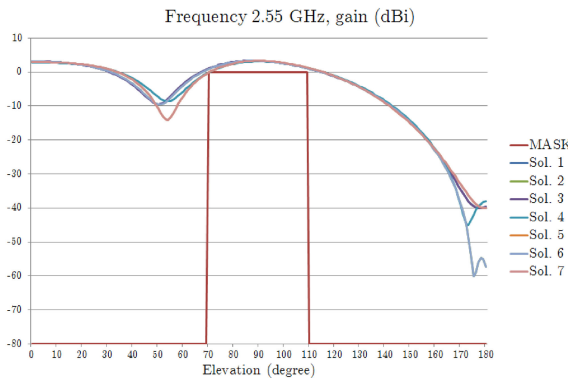


Figure 22.
2.55-GHz gain objective results using NSGA-II.

CONCLUSIONS AND FUTURE WORK

In this paper, we presented a simulation–optimization approach to the design of helical antennas. This is a very complex problem with several restrictions that must be met in two frequencies and, additionally, compacting the antenna dimensions as possible. To address the problem, we used two well-known multiobjective algorithms and still state-of-the-art algorithms, NSGA-II and SPEA-2, that were capable of improving the time and effort needed to find

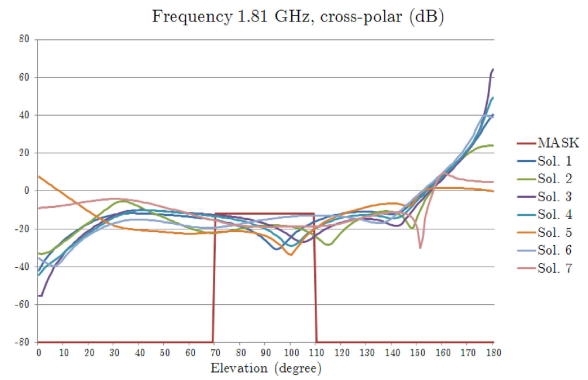


Figure 23.
1.81-GHz cross-polar objective results using SPEA-2.

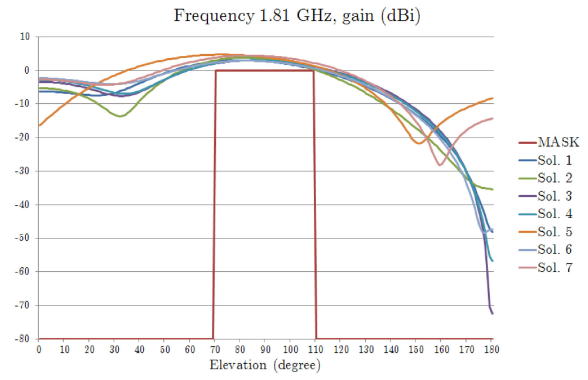


Figure 24.
1.81-GHz gain objective results using SPEA-2.

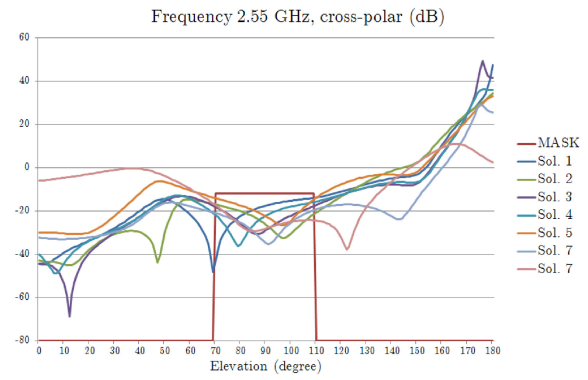


Figure 25.
2.55-GHz cross-polar objective results using SPEA-2.

valid solutions (antenna shape and dimensions) when compared with finding solutions using the GD as a searching technique together a simulator tool. The use of multiobjective algorithms reduced the time cost of algorithm execution when compared with a previous approach using the GD. Also, the simulation–optimization approach allow us to obtain multiple correct solutions that provide some flexibility and can help us to choose the final design of the antenna. Having more solutions, with different dimensions but all optimal from the radiation point of view, offers more

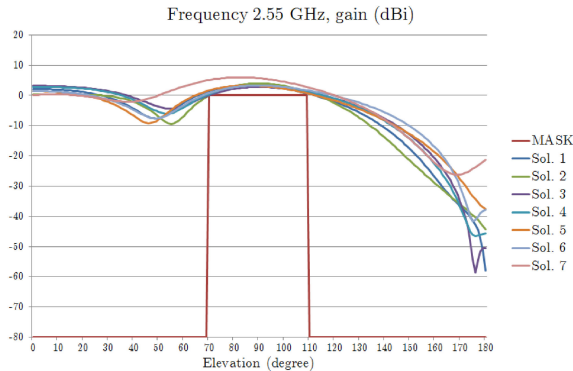


Figure 26.
2.55-GHz gain objective results using SPEA-2.

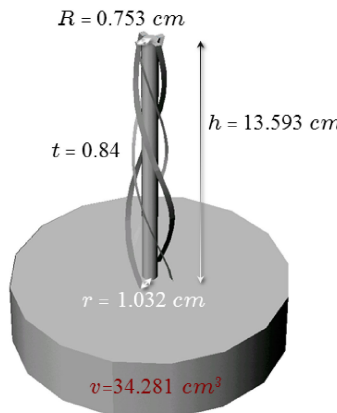


Figure 27.
Geometrical model of the solution with a lower volume (SPEA-2.5).

possibilities for the manufacturing not only for the antenna but the rest of elements that are coupled closely to it.

Future works include the use other multiobjective algorithms capable of handling the constraints to compare and adapt them to the difficulty of this problem. We will also explore many-objective algorithms as we are handling five objectives in this paper.

ACKNOWLEDGMENT

This work was supported by the University of Alcalá, Projects BadgePeople (TIN2016-76956-C3-3-R), and the Spanish Department of Science, Innovation and Universities, Project TEC2017-89456-R.

REFERENCES

- [1] I. González, E. García, F. Sáez de Adana, and M. F. Cátedra, “Monurbs: A parallelized multipole multilevel code for analyzing complex bodies modeled by nurbs surfaces,” *Appl. Comput. Electromagn. Soc. J.*, vol. 23, no. 2, pp. 134–142, 2008.
- [2] K. Deb, A. Pratap, S. Agarwal, and T. Meyarivan, “A fast and elitist multiobjective genetic algorithm: NSGA-II,” *IEEE Trans. Evol. Comput.*, vol. 6, no. 2, pp. 182–197, Apr. 2002.
- [3] E. Zitzler, M. Laumanns, and L. Thiele, “SPEA2: Improving the strength pareto evolutionary algorithm,” *Comput. Eng. Netw. Lab.*, Swiss Federal Inst. Technol., Zürich, Switzerland, Tech. Rep. 103, 2001.
- [4] I. González, J. Gómez, A. Tayebi, and M. F. Cátedra, “Optimization of a dual-band helical antenna for TTC applications at s band,” *IEEE Antennas Propag. Mag.*, vol. 54, no. 4, pp. 63–77, Aug. 2012.
- [5] J. Moreno, I. Gonzalez, and D. Rodriguez, “Using simulation and the NSGA-II evolutionary multi-objective algorithm in the design of a compact dual-band equatorial helix antenna,” in *Proc. 6th Int. Conf. Space Mission Challenges Inf. Technol.*, Sep. 2017, pp. 56–60.
- [6] P. Sumithra and D. Thiripurasundari, “A review on computational electromagnetics methods,” *Adv. Electromagn.*, vol. 6, no. 1, pp. 42–55, 2017.
- [7] C. A. Balanis, *Advanced Engineering Electromagnetics*. Hoboken, NJ, USA: Wiley, 1989.
- [8] R. G. Kouyoumjian, “Asymptotic high-frequency methods,” *Proc. IEEE*, vol. 53, no. 8, pp. 864–876, Aug. 1965.
- [9] R. G. Kouyoumjian and P. H. Pathak, “A uniform geometrical theory of diffraction for an edge in a perfectly conducting surface,” *Proc. IEEE*, vol. 62, no. 11, pp. 1448–1461, Nov. 1974.
- [10] J. A. Stratton, *Electromagnetic Theory*. New York, NY, USA: MacGraw-Hill, 1941.
- [11] P. Y. Ufimtsev, “Elementary edge waves and the physical theory of diffraction,” *Electromagnetics*, vol. 11, no. 2, pp. 125–160, 1991.
- [12] W. Chew, E. Michielssen, J. M. Song, and J. M. Jin, Eds., *Fast and Efficient Algorithms in Computational Electromagnetics*. Norwood, MA, USA: Artech House, 2001.
- [13] O. L. Zienkiewich, *The Finite Element Method*. New York, USA: MacGraw-Hill, 1979.
- [14] A. Taflove, “Application of the finite-difference time-domain method to sinusoidal steady-state electromagnetic-penetration problems,” *IEEE Trans. Electromagn. Compat.*, vol. EMC-22, no. 3, pp. 191–202, Aug. 1980.
- [15] “Computational-electromagnetics research group.” 2018. [Online]. Available: <https://www.uah.es/en/investigacion/unidades-de-investigacion/grupos-de-investigacion/Computacional-electromagnetics/#Miembros>.
- [16] G. Farin, *Curves and Surfaces for Computer Aided Geometric Design: A Practical Guide*. New York, NY, USA: Academic, 1988.
- [17] J. M. Garrido, M. A. Díaz, I. G. Diego, and M. F. Cátedra Pérez, “Design and evaluation of the multilevel mesh generation mode for computational electromagnetics,” *Appl. Comput. Electromagn. Soc. J.*, vol. 30, no. 6, pp. 578–588, 2015.

- [18] H. A. van der Vorst, “Bi-CGSTAB: A fast and smoothly converging variant of bi-CG for the solution of nonsymmetric linear systems,” *SIAM J. Sci. Statist. Comput.*, vol. 13, no. 2, pp. 631–644, Mar. 1992. [Online]. Available: <http://dx.doi.org/10.1137/0913035>
- [19] Y. Saad and M. H. Schultz, “GMRES: A generalized minimal residual algorithm for solving nonsymmetric linear systems,” *SIAM J. Sci. Statist. Comput.*, vol. 7, no. 3, pp. 856–869, Jul. 1986. [Online]. Available: <http://dx.doi.org/10.1137/0907058>
- [20] C. A. C. Coello, “A comprehensive survey of evolutionary-based multiobjective optimization techniques,” *Knowl. Inf. Syst.*, vol. 1, pp. 269–308, 1998.
- [21] N. Srinivas and K. Deb, “Multiobjective optimization using nondominated sorting in genetic algorithms,” *Evol. Comput.*, vol. 2, pp. 221–248, Sep. 1994. [Online]. Available: <http://dx.doi.org/10.1162/evco.1994.2.3.221>
- [22] “Dxf reference,” 2012. [Online]. Available: http://images.autodesk.com/adsk/files/autocad_2012_pdf_dxf-reference_en%u.pdf
- [23] “Fasant.” 2018. [Online]. Available: <http://www.fasant.com>
- [24] E. García, C. Delgado, I. G. Diego, and M. F. Cátedra, “An iterative solution for electrically large problems combining the characteristic basis function method and the multilevel fast multipole algorithm,” *IEEE Trans. Antennas Propag.*, vol. 56, no. 8, pp. 2363–2371, Aug. 2008.
- [25] C. Delgado, M. Cátedra, and R. Mittra, “Application of the characteristic basis function method utilizing a class of basis and testing functions defined on nurbs patches,” *IEEE Trans. Antennas Propag.*, vol. 56, no. 3, pp. 784–791, Mar. 2008.
- [26] C. Delgado, M. F. Cátedra, and R. Mittra, “Efficient multi-level approach for the generation of characteristic basis functions for large scatters,” *IEEE Trans. Antennas Propag.*, vol. 56, no. 7, pp. 2134–2137, Jul. 2008.
- [27] “MPI and OpenMP introduction,” 2018. [Online]. Available: <http://www.hpc.cineca.it/content/introduction-parallel-computing-mpi-an% d-openmp>
- [28] A. J. Nebro, J. J. Durillo, and M. Vergne, “Redesigning the jmetal multi-objective optimization framework,” in *Proc. Companion Publication Annu. Conf. Genetic Evol. Comput.*, 2015, pp. 1093–1100. [Online]. Available: <http://doi.acm.org/10.1145/2739482.2768462>

HARWIN

Higher Reliability smaller footprint

New Ready-To-Use Cable Assemblies

Now Available with Reverse Fixing Screw-Lok for Design Flexibility

- Save time and money on tooling, training and testing cables
- Metal back-shells for maximum strain relief and RF shielding
- Up to 45% smaller and up to 75% lighter than Micro-D
- Resists extremes of shock, vibration and temperature
- Excellent out-gassing properties

gecko **SL**

www.harwin.com/gecko-sl